Research Article BEU Fen Bilimleri Dergisi 15(1): 97-113 (2026) DOI: 10.17798/bitlisfen.1759027

BİTLİS EREN UNIVERSITY
FEN BİLİMLERİ DERGİSİ
ISSN: 2147-3129 / e-ISSN: 2147-3188

FLOATING PV DISTRIBUTED GENERATION SYSTEM PROPOSAL AND OPTIMAL LCL FILTER DESIGN FOR AKKÖPRÜ DAM, MUĞLA, TURKEY

Alp KARADENİZ

Balikesir University, Electrical & Electronics Engineering Department, Balıkesir, Türkiye, akaradeniz@balikesir.edu.tr

Article Info

Received: *August 5, 2025*
Revised: *December 1, 2025*
Accepted: *January 23, 2026*

Keywords
Solar energy,
Floating photovoltaic DGU,
Power quality,
Optimization,
Passive Filters.

ABSTRACT

The study investigates the burgeoning potential of floating photovoltaic (FPV) panels and proposes their installation in Akköprü Dam, Muğla, Turkey. Also, different kinds of power electronics-based converters and inverters are used in the grid integration of FPV. These electrical gadgets cause harmonics in voltage and current waveforms to be introduced into the grid. Therefore, a 2 MW FPV system is designed to be combined and connected to the 120 kV common grid by a 25 kV distribution feeder. This research examines optimal passive filter designs and harmonic analysis for FPV power systems. Also, utilising real-world meteorological data that is taken from Dalaman, Muğla, Turkey, such as solar irradiation, as an input parameter of the FPV. After that, to study harmonic analysis and optimal filter design, a mathematical strategy is proposed. Moreover, the arithmetic mean (AM) of real data is considered the input value of FPV. Also, to discover the best filter solution, the Antlion Optimisation (AOA) algorithm is used. According to IEEE 519 standards, the optimisation method seeks to minimise both the voltage levels in p.u. and the total harmonic distortion (THD) of current and voltage values. Moreover, the FPV model is simulated with optimal LCL filters by using daily data (DD) solar irradiation values. Finally, the performance analysis based on the results of AM data and DD is studied. Lastly, the results are comparatively discussed.

1. INTRODUCTION

The recent studies evaluating FPV implementations across diverse climates and reservoir types worldwide report enhanced energy yield, cooling-effect benefits, and water-energy synergy under variable irradiance and thermal conditions [1]–[3]. Turkey currently finds itself in a situation of energy dependency. In 2017, renewable sources accounted for 43.27% of the total installed capacity for power generation, leaving the remainder reliant on fossil fuels, which possess a restricted reserve. This scenario poses significant environmental concerns and heightens external reliance. Conversely, renewable resources offer a sustainable and environmentally friendly alternative, particularly through recent developments in wind and solar energy [4]. The total installed capacity in Turkey is on the rise, and the proportion of solar power within Turkey's overall electricity capacity is also increasing. Each year, the supply rate experiences growth due to both operational power plants and those currently being constructed (refer to Table 1). In 2023, Turkey witnessed an increase in total additional installed capacity, reaching 2,859 MW, primarily driven by wind and solar energy, which constituted 99.4% of the total increment. The nation’s renewable energy portfolio reached 59.21 GW, including nearly 32.1 GW of hydropower, while wind and solar contributed 11.82 GW and 11.33 GW, respectively [5].

Solar power is increasingly becoming a notable contributor to renewable energy in Turkey, owing to its abundant solar energy potential. Over the last decade, substantial investments have been made in photovoltaic solar plants, resulting in a deployed capacity of 6.2 GW as of June 2020, with continued growth anticipated [6]. A global trend in solar power involves the deployment of solar panels on bodies of water such as lakes and dam reservoirs, offering various advantages, including the preservation of

fertile land, reduction of evaporation, and provision of natural cooling for the panels. Floating PV systems bring numerous benefits, such as heightened system efficiency and diminished water evaporation on dams and reservoirs. Leveraging water bodies for cooling purposes can maintain lower panel temperatures compared to land-based installations, thereby increasing overall efficiency. Additionally, floating PV systems provide shading to the water's surface, further reducing evaporation and safeguarding freshwater supplies, making them a valuable renewable energy solution [7].

Table 1: Installed solar power yearly capacities of Turkey (2014-2023).

Year	Total installed capacity of Solar power (MW)
2014	69520
2015	73147
2016	78497
2017	85200
2018	91733
2019	95167
2020	100413
2021	104644
2022	105300
2023	113661

In recent times, Turkey has observed an increasing enthusiasm for floating photovoltaic (FPV) ventures, marked by numerous trial endeavours and exploratory examinations throughout the nation. These initiatives vary from minor installations on reservoirs to extensive, large-scale implementations on inland lakes and coastal regions. As advancements in technology progress and expenses diminish, FPV is anticipated to assume a progressively vital position in Turkey's shift towards renewable energy, bolstering the country's energy stability, economic advancement, and ecological resilience [8].

Various power electronics-based converters and inverters are utilised for integrating floating photovoltaic (FPV) systems into the grid, leading to the introduction of harmonics into voltage and current waveforms. These harmonics can trigger issues like transformer overheating, circuit breaker tripping, and compromised equipment lifespan, necessitating a focus on minimizing them to maintain power quality standards aligned with guidelines such as IEEE 519-2014 and IEC 61000 [9]. Additionally, the chosen region, Akköprü Dam, is favourable for solar power generation systems due to its high solar irradiation capture potential, further supporting the integration of FPV units into the grid [10].

In this paper, the optimal design of a series LCL filter [11], which can effectively be used for high-frequency harmonics, is studied for systems including FPV for arithmetic mean (AM) values of hourly data obtained from the European Commission for Akköprü Dam, Muğla [10]. First of all, an objective function (OF) that includes the total harmonic distortion of the voltage waveform (THDV), the effective value of the voltage magnitude, and the power of the passive filter is created. To find optimal filter parameters, a meta-heuristic optimisation algorithm recently proposed in the literature, the Antlion Optimisation Algorithm (AOA) algorithm [12], is employed to solve OF. In addition, filter parameter effects on system performance with respect to power quality essentials (THD, voltage level, power factor, and power values) are studied, and performance analysis for between AM and DD input with an optimal filter is given in the study.

1.1. Literature Overview

According to the literature summary, there are some studies about FPV installations in Turkey [13–19]. In one of these studies, the study [18] demonstrates the application of floating photovoltaic solar power systems in Burdur, employing methodologies like Analytic Hierarchy Process and Weighted Linear Combination and utilising input layers such as global horizontal irradiance, wind speed, elevation, and power networks to generate discriminated and compound FPV suitability maps for water bodies. It underscores the significance of hybrid investments and energy islands to mitigate water-related risks, focusing on large, deep, and calm water bodies like Burdur Lake and Karacaoren I Dam Reservoir to ensure safer options for investors.

Also, the study [14] assesses the potential for floating photovoltaics (FPV) on the expansive water surfaces of hydroelectric power plants (HEPPs) in Turkey, utilising the Random Forest algorithm to determine surface areas and evaluating FPV technical potential across various scenarios. Results indicate substantial FPV technical potential, reaching 380,439.85 MW and recovering 25.40 km3/year of water when utilising entire dam surfaces, meeting a significant portion of Turkey's total installed power capacity and demonstrating the vast untapped potential of FPV solar power plants on HEPPs' idle water surfaces.

In addition to that, the study [13] investigates the challenges and critical faults associated with floating photovoltaic (FPV) systems based on three installations on Büyükçekmece Lake in Istanbul, ranging from 9 kWp to 90 kWp. Findings reveal that warpage due to harsh wave action poses a significant issue, and while previously installed systems faced durability issues, the new 30 kWp FPV designs proved robust and sustainable even under severe wind and wave conditions. The research underscores the importance of flexibility at the system level and stability at the individual unit level for effective FPV designs.

Moreover, the study [17] proposes a new method for selecting optimal sites for floating photovoltaic (FPV) systems on water reservoirs by analysing long-term area and shoreline changes alongside annual and monthly total global horizontal irradiance values. Utilising remote sensing and geographic information system tools, the research underscores the importance of considering land topography and shading patterns to identify the most efficient locations for FPV solar power plants (SPPs) on water surfaces.

Also, the manuscript [19] delves into the growing significance of floating photovoltaic (PV) systems as a promising technology in solar energy utilisation, examining their potential impact on energy generation, environmental sustainability, and economic feasibility. With a surge in global demand for renewable energy, innovative approaches like floating solar farms, or FPV, are gaining traction, showcasing the advantages and disadvantages of integrating solar panels on water bodies such as lakes, ponds, reservoirs, and seas.

Additionally, the paper discusses [15] the significance of advancing solar power technologies, highlighting floating photovoltaic panels (FPV) as a solution for expedited deployment, reduced maintenance costs, and enhanced efficiency compared to land-based installations. Focused on Romania's solar energy potential, the study assesses three lakes in Romania's eastern region to the western Black Sea coast, utilising the ERA5 database and in situ measurements to reveal high solar energy exploitation potential and minimal disparities between the database and measured solar radiation values.

Moreover, in study [20] Solar-PV systems are widely used for converting solar energy into electricity, but challenges like partial shading (PS) and harmonics impact their performance and power quality. PS causes issues such as hot spots and multiple peaks in the power-voltage curve, requiring modifications in MPPT techniques. A PSCAD/EMTDC-based model demonstrates a modified Incremental Conductance (INC) technique for effective MPP tracking under PS conditions, along with an analysis of harmonics and mitigation strategies.

Additionally, the study [21] provides a concise review of floating PV technology and its efficiency-enhancing mechanisms. The study highlights cooling effects and increased irradiance over water surfaces. It also summarizes recent FPV deployment trends across different regions.

Also, the study [22] evaluates FPV performance across 4,244 water bodies under diverse climate conditions. The results show notable gains in energy yield and evaporation reduction. The work demonstrates FPV’s potential for large-scale energy–water integration.

In addition to that, in study [23] present a global review of LCL filter design for grid-connected converters. The study outlines key stability, resonance and harmonic-attenuation considerations. It also summarizes modern optimization strategies used in renewable energy interfaces.

Lastly the study [24] analyze global FPV installation trends and environmental impacts. Their results indicate enhanced performance and promising sustainability characteristics. The study also identifies major engineering and ecological factors influencing FPV expansion.

1.2. Motivation

From the literature summary presented here, it can be mentioned that studies on FPV systems have gained importance in the recent literature. In addition, recent studies [14,17,19] have focused on the FPV power generation capacity of Turkey. However, currently, there is no study about the application of the FPV system for Akköprü Dam in Turkey. Also, in the literature, studies [7,9,12] discuss the analysis, capacity, shadow effect, and location proposal for FPV in Turkey, but the harmonic effects of FPV on the grid have not been investigated using DD. In this regard, this study is novel. Additionally, the technique for optimal filter design with AM data and the performance analysis of the filter under DD have never been studied in the literature.

1.3. Contributions to the knowledge

In this paper, some important contributions are provided:

- The proposed FPV system is simulated for arithmetic mean (AM) values of DD obtained from the European Commission for Muğla, Turkey.
- For an objective function (OF) including the total harmonic distortion of the voltage waveform (THDV), the system's rms voltage levels, and the harmonic distortion constraints, the optimal design of the passive filter type, series LCL filters, is formulated.
- To find optimal parameters of the considered filter type according to the formulated problem, a meta-heuristic optimization algorithm recently proposed in the literature, the Antlion Optimization Algorithm (AOA) algorithm, is employed.
- The technique for optimal filter design with AM data is proposed in the study.
- The performance analysis with respect to power quality essentials (THD, voltage level, power factor, and power values) of the filter under DD is studied.

2. MODELLING OF THE STUDIED SYSTEM

In this section, the modelling of the studied system is introduced.

2.1. Modelling of power system

The schematic of the studied system containing 2 MW FPV power system is given in Figure 1. It has a 120 kV Grid system, a 120/25 kV transformator wye/delta connected 47 MVA, a 25kV/575V transformator delta/wye connected 2.5 MVA power system.

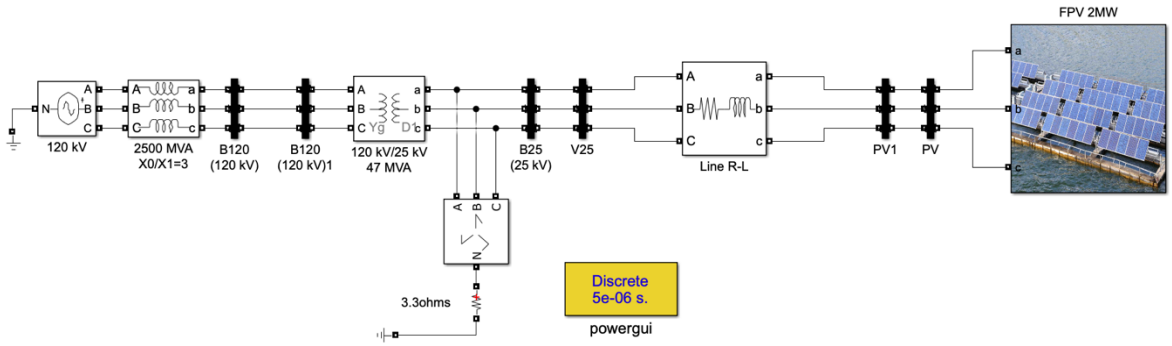

Figure 1: The Simulink model of FPV power system.

In the system, there are two power transformers. Model parameters of both transformers are shown in Figure 2. It is seen from this figure that the first one has nameplate properties such as 120/25 kV, 50 Hz, wye/delta connection, and 47 MVA. The resistances and inductances of its windings and magnetization inductance are 0.0027 p.u, 0.08 p.u and 500 p.u. In addition, the second one has nameplate properties such as 2.5kV/575V, delta/wye connection, and 2.5 MVA. The resistances and inductances of its primary winding are 8.33 $x10^{-4}$ p.u. and 0.025 p.u, those parameters for secondary winding are $8.33x10^{-4}$ p.u and 0.08 p.u, and its magnetization inductance is 500 p.u.

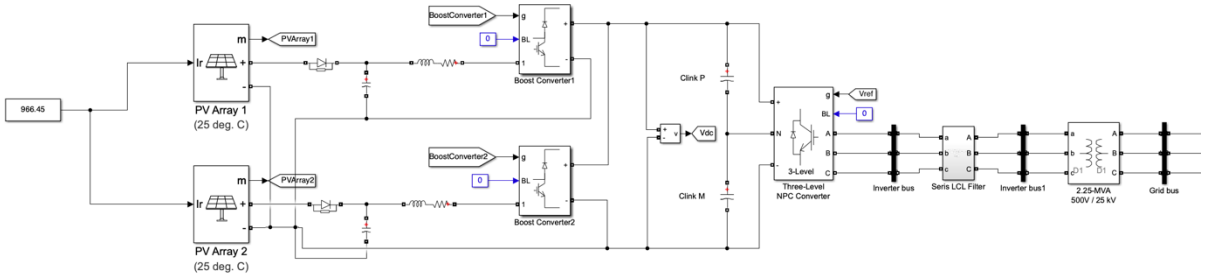

Figure 2: Under mask illustration of PVDGU solar system block.

In a combined modelled framework, a 2 MW Photovoltaic Distributed Generation Unit (PVDGU) is central, with two PV arrays, PV Array 1 and PV Array 2, generating 1.5 MW and 500 kW respectively under specific environmental conditions. Each array connects to a boost converter regulated by Maximum Power Point Trackers (MPPT), optimizing power extraction. The output from the boost converters is linked to a shared 1000 V DC bus, which is then transformed to approximately 500 V AC by a three-level Neutral Point Clamped (NPC) converter before coupling to the grid via a 2.25-MVA transformer. Moreover, The FPV arrays employ the Perturb and Observe (P&O) MPPT algorithm implemented in MATLAB/Simulink, which adjusts the duty cycle of the boost converter to track the maximum power point under varying irradiance. In addition to that, the overall FPV–LCL system, including the power stage and its control loops, is implemented in MATLAB/Simulink as shown in Figure 1-2, following similar modelling practices adopted in recent grid-connected PV and hybrid RES studies [25]-[27]. Also, the DC–DC boost converters are implemented using the switching-devices model in MATLAB/Simulink, and their main design parameters (inductance, output capacitance, switching frequency, on-state resistance and snubber elements) are summarized in Table 2.

Table 2. Electrical and Switching Parameters of the DC–DC Boost Converter

Parameter	Symbol	Value	Description
IGBT on-state resistance	R_on	1×10^{-4} Ω	Internal conduction resistance of the switch
Diode forward voltage	V_F,diode	0 V	Ideal diode behaviour in Simulink model
IGBT forward voltage	V_F,IGBT	0 V	Ideal switch characteristic
Snubber resistance	R_sn	1×10^{6} Ω	High-value snubber resistance (passive)
Snubber capacitance	C_sn	∞	Snubber capacitors disabled
Model type	—	Switching devices	Detailed IGBT + diode switching model
Duty-cycle input	D	From MPPT	Duty ratio generated by P&O MPPT algorithm

2.2. Data preparation process for Akköprü Dam

This paper conducts a performance analysis of the modelled system using the standard meteorological year (TMY) dataset sourced from the European Commission, Joint Research Centre (JRC). The TMY dataset encompasses the period from March 2005 to June 2020, spanning approximately 15 years, with hourly data available. It comprises the solar irradiance, data. Furthermore, sample data from Akköprü Dam, situated in Muğla region, is considered [10]. The geographical coordinates of the pivot point are latitude 36.897 and longitude 28.907 for the Akköprü Dam area. Figure 3 illustrates the geological position of the pivot point within the Muğla region.

This paper conducts a performance analysis of the modelled system using the standard meteorological year (TMY) dataset sourced from the European Commission, Joint Research Centre (JRC). The TMY dataset encompasses the period from March 2005 to June 2020, spanning approximately 15 years, with hourly data available. It comprises the solar irradiance, data. Furthermore, sample data from Akköprü Dam, situated in Muğla region, is considered [10]. The geographical coordinates of the pivot point are latitude 36.897 and longitude 28.907 for the Akköprü Dam area. Figure 3 illustrates the geological position of the pivot point within the Muğla region.

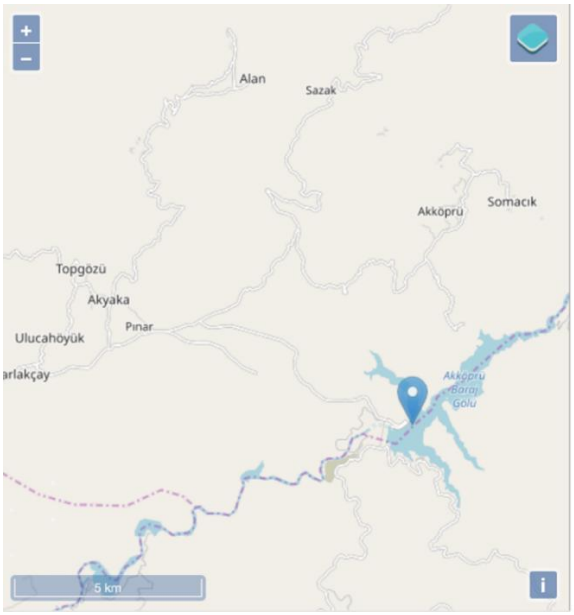

Figure 3: The geological location of pivot point Akköprü Dam area.

In addition to that, Akköprü Dam, which is the largest dam in the Aegean Region and the 6th largest dam in Turkey, started construction in 1996 and was opened on May 27, 2011, costing 1.4 billion Turkish Lira. The dam is located on the Dalaman River, 24 km east of Köyceğiz, Muğla District. With 384 million cubic meters of water to be stored in the dam, it has the capacity to irrigate 1,419,200 hectares of land and produce 343 million kWh of energy annually with a power plant of 118.6 MW installed capacity. The hydropower data of Akköprü Dam with rating values of Muğla and Turkey are given at Table 3 annually [28].

Table 3: The performance analysis of Akköprü Dam (2012-2023)

Year	Production (kWh)	Ratio to Muğla consumption (%)	Ratio to Turkey consumption (%)
2012	207.000.000	5,7	0,09
2013	285.015.000	7,7	0,12
2014	199.956.000	5,2	0,08
2015	430.506.000	11%	0,16
2016	120.255.800	2,9	0,043
2017	121.651.000	2,8	0,042
2018	132.587.000	2,9	0,044
2019	198.324.450	4,3	0,07
2020	124.016.310	2,7	0,041
2021	90.839.830	1,9	0,028
2022	144.782.240	3,1	0,044
2023	78.410.330	1,6	0,024

Akköprü Dam is selected due to its favourable solar irradiance, making it an ideal location for FPV system installation in Akköprü Dam (Figure 4). Notably, there are currently no FPV system applications at Akköprü Dam. Hence, a secondary objective of this study is to identify potential FPV system application areas within Muğla. Furthermore, the model is simulated over a 20-second scale, representing daily values for one month in the Akköprü Dam dataset for June 2020. This entails the linear scaling of 744 data points over the 20-second timeframe, resulting in a time representation of 0.02688 seconds per data point. The nominal power value for the FPV system is set at 2 MW, corresponding to a weather degree of 25 and a solar irradiation value of 1000 W/m2. However, to reflect application performance, an optimal passive filter design is developed based on the arithmetic mean value (966.45 W/m2) derived from the solar irradiation data points for June 2020. Table 4 presents the

nominal and AM data for the FPV system. In this study, AM data is utilised to formulate an optimal design and conduct performance analysis.

Figure 4: Akköprü Dam, Muğla [29].

Table 4: Data scaling of AM data for optimal filter design.

	Nominal data	**AM data**
Solar irradiation	1000 W/m2	966.45 W/m2
FPV system power	2 MW	1.932 MW

As seen from Table 4, the nominal and AM data of the FPV system's powers are 2 MW and 1.932 MW, respectively. Also, while the optimal filter performance analysis is done using DD, DD is considered every day at 10 a.m. for 30 days.

2.3. Harmonic analysis of the FPV studied system without filter

Figure 5 and Figure 6 show the waveforms and harmonic spectrums of the voltage and current at PV and 25 kV buses for the system without the passive filter, respectively. From Table 5, the THDV (%) values of the PV and 25 kV buses are 5.23% and 5.12%, and the THDI (%) values of the buses are 10.65% and 10.66%. In addition to that, Vpu values of the buses 1.07 p.u and 1.06 p.u. Thus, one can see that the system without a filter has highly distorted voltage and currents, and their THD values are over the limits defined by the IEEE-519 standards [30] given in Table 6.

Table 5: The THDV (%), Vpu and THDI (%) values of the PV and 25 kV buses.

THDV(%)	
25kV Bus	5.12 %
PV Bus	5.23 %
Vpu	
25kV Bus	1.06 p.u
PV Bus	1.07 p.u
THDI(%)	
25kV Bus	10.65 %
PV Bus	10.66 %

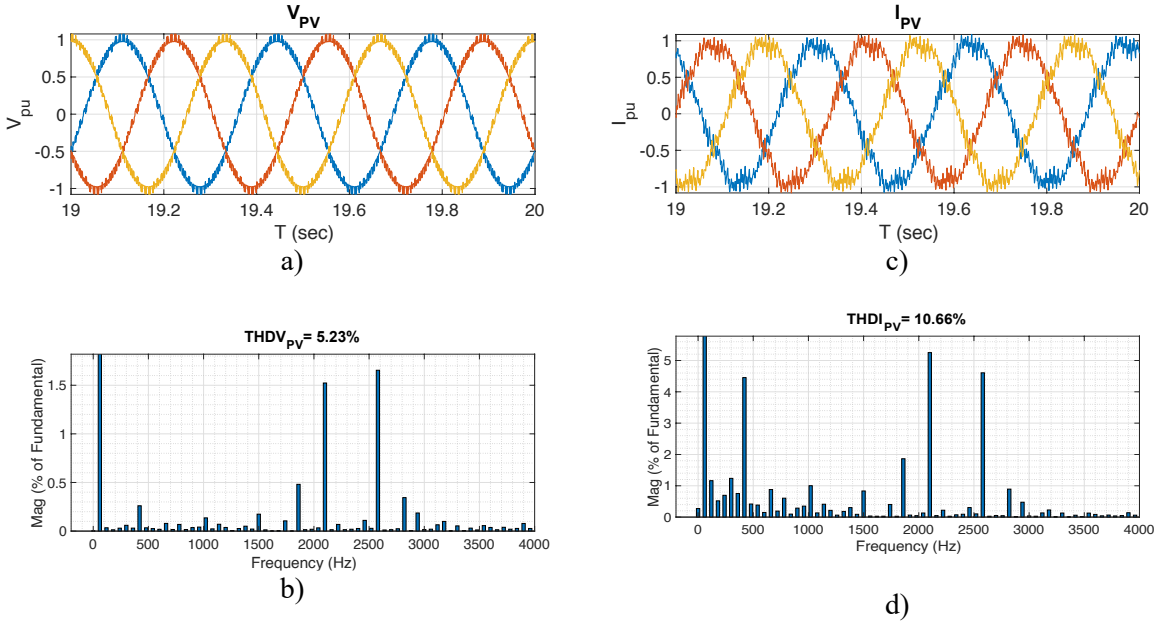

Figure 5: The (a) voltage waveforms, (b) voltage harmonic spectrums, (c) current waveforms and (d) current harmonic spectrums at the PV bus for the system without the filter.

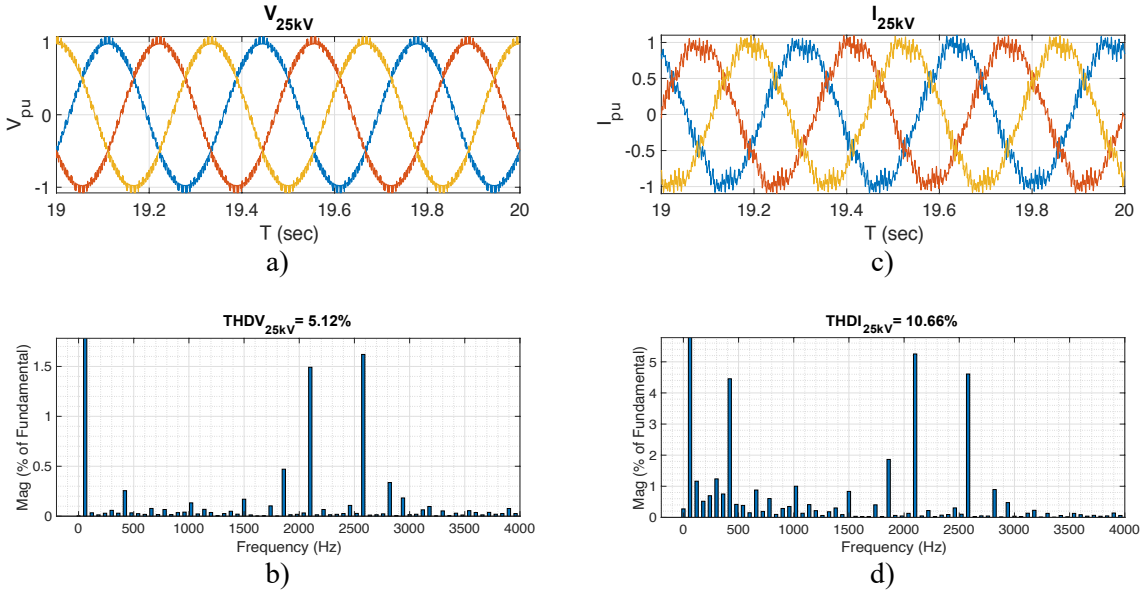

Figure 6: The (a) voltage waveforms, (b) voltage harmonic spectrums, (c) current waveforms and (d) current harmonic spectrums at the 25kV bus (PCC) for the system without the filter.

Table 6: The IEEE std. 519 harmonic limits.

Bus Voltage V at PCC	Individual Harmonic (%)	Total Harmonic Distortion THD (%)
V ≤ 1.0 kV	5.0	8.0
1 kV < V ≤ 69 kV	3.0	5.0
69 kV < V ≤ 161kV	1.5	2.5
161kV < V	1.0	1.5

3. FORMULATION AND SOLUTION ALGORITHM OF THE OPTIMAL FILTER DESIGN

In this section, the series LCL filter considered for harmonic mitigation in the system. Also, the optimal design of these filters is formulated, and the algorithm is introduced to solve the associated optimization problem.

3.1. Introduction to series LCL passive filter

In this study, the series LCL filter, which have high compensation capability for high-frequency harmonics, is chosen. Regarding their equivalent circuits given in Figure 7, the filter is briefly introduced below [11]:

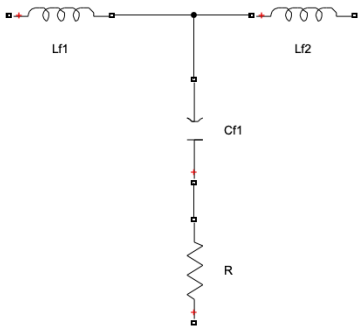

Figure 7: The single-phase representations series LCL filters.

The LCL filter configuration is widely employed as an interface between converters and the utility grid due to its efficacy in smoothing converter output currents. Moreover, it demonstrates superior performance with relatively small inductor and capacitor values. The LCL filter offers enhanced attenuation of higher harmonics, enabling operation at lower switching frequencies while adhering to harmonic constraints specified in standards like IEEE-519 and IEEE-1547 [31]. Also**,** a series LCL filter consists of three main components: the inverter-side inductor, the grid-side inductor, and the filter capacitor. Designing these three elements for an LCL filter typically involves solving three or more simultaneous equations, indicating the presence of multiple design objectives. But in this paper, the parameters (*Lf1, Lf2*, *Cf1* and *R*) of the series LCL filter are determined by AOA.

3.2. Problem formulation

The parameters of the series LCL passive filter are optimized to find the best suitable filter form to get a less harmonically polluted operating system. In addition to that, the voltage levels for all buses should be around 1 p.u. Also, the objective function is created with respect to the THDV, Vpu and power of filter loss values of the PV bus. The PV bus is selected as a candidate because it is the closest bus to the harmonic-producing source (PVDGU) of the system. The objective function of the optimization problem can be written as follows:

Objective Function:

$$\text{minimize} \quad F(obj) = a * THDV + b * \left|V_{pu} - 1\right| + c * \left|filter_{powerloss}\right|$$

Subject to:

$THDV_{h-individual} \leq Max\ THDV_{individual}$

$THDI_{h-individual} \leq Max\ THDI_{individual}$

$THDV_{\%} \leq Max\ THDV_{\%}$

$THDI_{\%} \leq Max\ THDI_{\%}$

a, b and c are coefficents of $THDV$, V_{pu} and $filter_{powerloss}$. $THDV$ is values of total harmonic distoriton of voltage. V_{pu} is p.u. value of a phase to ground voltage value of the buses. For this study, after

normalizing magnitudes of $THDV$, V_{pu} and $filter_{powerloss}$ a, b and c are choosen as; 0.4, 0.3 and 0.3. $filter_{powerloss}$ is power values of series LCL filter which are optimally found. $Max\ THDV_{individual}$ and $Max\ THDI_{individual}$ values are individual harmonic limits for voltage and current values restricted by IEEE 519 standarts. $THDV_{h-individual}$ and $THDI_{h-individual}$ are hth harmonic values of current and voltage. Also, $Max\ THDV_{\%}$ and $Max\ THDI_{\%}$ are determined by IEEE 519 standarts with respect to suitable voltage levels.

3.3. Solution algorithm

To determine the optimal filter parameters, we utilize a meta-heuristic optimization algorithm called the Antlion Optimization Algorithm (AOA) [12] and the algorithm is introduced below.

3.3.1. Antlion optimization algorithm (AOA)

The Antlion Optimization Algorithm mimics the hunting behaviour of antlions, where larvae create traps resembling conical paths to ensnare ants, their prey. By hurling grains of sand to hinder escape and draw prey towards the trap's bottom, antlions quickly consume ensnared ants using their robust mandibles before resetting the trap for new arrivals [12].

In formulating the algorithm, the mathematical representation of the random movements of ants is articulated in the manner presented in Eq. (1). In this equation, *n* denotes the maximum number of iterations, *t* denotes random walk steps (iteration count), *cumsum* denotes the cumulative sum of steps, and *r(t)* represents a random function. The stochastic function *r(t)* can be expressed as delineated in Eq. (2). According to this expression, when *rand* is less than or equal to 0.5, the value of *r(t)* is zero, and when rand exceeds 0.5, the value of *r(t)* is 1 [12].

$$X(t) = \begin{pmatrix} 0 \\ cumsum(2r(t_1) - 1) \\ cumsum(2r(t_2) - 1) \\ . \\ . \\ . \\ cumsum(2r(t_n) - 1) \end{pmatrix} \tag{1}$$

$$\text{r(t)} = \begin{cases} 1\ if\ rand\ > 0.5 \\ 0\ if\ rand\ \leq 0.5 \end{cases} \tag{2}$$

On the flip side, while updating the positions of ants during their random walks to ensure they remain within the boundaries of the search space, their positions are standardized in accordance with the expression furnished in Eq. (3). Here, *i* represents the number of variables, a_i represents the minimum random walk of the i[th] variable, c_i^t and d_i^t signify the minimum and maximum values of the i[th] variable at the t[th] iteration.

$$X_i^t = \frac{(X_i^t - a_i)(d_i - c_i^t)}{d_i^t - a_i} + c_i \tag{3}$$

Upon ants falling into the trap, the mathematical depiction of the sand-throwing motion executed by the antlion to draw them to the bottom of the trap is provided in Eq. (4)-(7). Moreover, *I* denote the shifting ratio [12].

$$c_{i=}^t\ Antlion_j^t + c^t \tag{4}$$

$$d_{i=}^t\ Antlion_j^t + d^t \tag{5}$$

$$c^t = \frac{c^t}{I} \tag{6}$$

$$d^t = \frac{d^t}{I} \tag{7}$$

The equation provided describes the new positions of ants walking around the ant lion selected by the roulette wheel and the elite ant lion. From Eq. (8), Ant_i^t represents the new position of the ith ant in the tth iteration. R_A^t denotes the random walk around the ant lion selected by the roulette wheel in the tth iteration, while R_E^t represents the random walk around the elite ant lion in the tth iteration.

$$Ant_i^t = \frac{R_A^t + R_E^t}{2} \tag{8}$$

In the last phase, subsequent to antlions consuming the ants that fell into the trap, they adjust their positions in accordance with the expression provided in Eq. (9). Here, $Antlion_j^t$ denotes the jth antlion at iteration t [12].

$$Antlion_j^t = Ant_i^t \quad if \quad f(Ant_i^t) < f(Antlion_j^t) \tag{9}$$

4. ANALYIS RESULTS

The AOA algorithm is executed in the Matlab/Simulink environments on a Mac OS operating system, utilizing a MacBook Pro with 16GB RAM and a 256GB SSD. Initially, an objective function (OF) is devised, incorporating factors such as the total harmonic distortion of the voltage waveform (THDV), the effective value of the voltage magnitude, and the power of the passive filter. The Antlion Optimization Algorithm (AOA) is employed to optimize the filter parameters. Moreover, the study assesses the influence of filter parameters on system performance, with a focus on power quality metrics such as THD, voltage levels, power factor, and power values. This analysis facilitates performance evaluations with DD and AM data comparisons.

4.1. Optimal LCL filter design process

To eliminate harmonics at PCC points, the meta-heuristic optimization algorithms (AOA) is used. The LCL filter parameters are listed in Table 7. For the system with the achieved optimal filters, the Vpu, THDVs and THDIs at the PV and 25 kV buses are presented in Table 7.

Table 7: The parameters of the optimal filter designs attained by AOA.

AOA	
Series LCL Filter	
X_{C1} (Ω)	2.6x105
X_{C2} (Ω)	-
X_{L1} (Ω)	0.0191
X_{L2} (Ω)	0.0078
R (Ω)	0.001

It is seen from Table 7 that, by using the AOA algorithm, optimal values of series LCL filter parameters, X_{C1}, X_{L1}, X_{L2}, R, are found as 2.65x10^5 Ω , 0.0191 Ω, 0.0078 Ω and 0.001 Ω respectively.

Moreover, Figure 8 and Figure 9 show the waveforms and harmonic spectrums of the voltage and current at PV and 25 kV buses for the system with the filter, respectively. From Table 5, the THDV (%) values of the PV and 25 kV buses are 1.02% and 1.00%, and the THDI (%) values of the buses are 2.27% and 2.26%. In addition to that, Vpu values of the buses 1.03 p.u and 1.02 p.u. Thus, one can see that the system with a filter has highly improved voltage and currents, and their THD values are stayed in limits defined by the IEEE-519 standards [30].

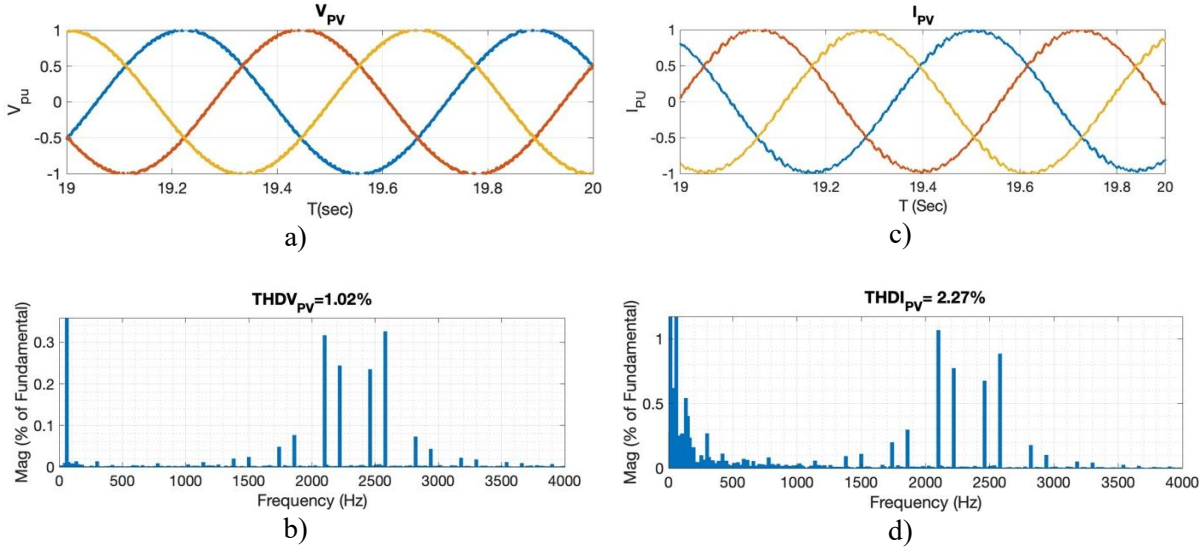

Figure 8: The (a) voltage waveforms, (b) voltage harmonic spectrums, (c) current waveforms and (d) current harmonic spectrums at the PV bus for the system with the filter.

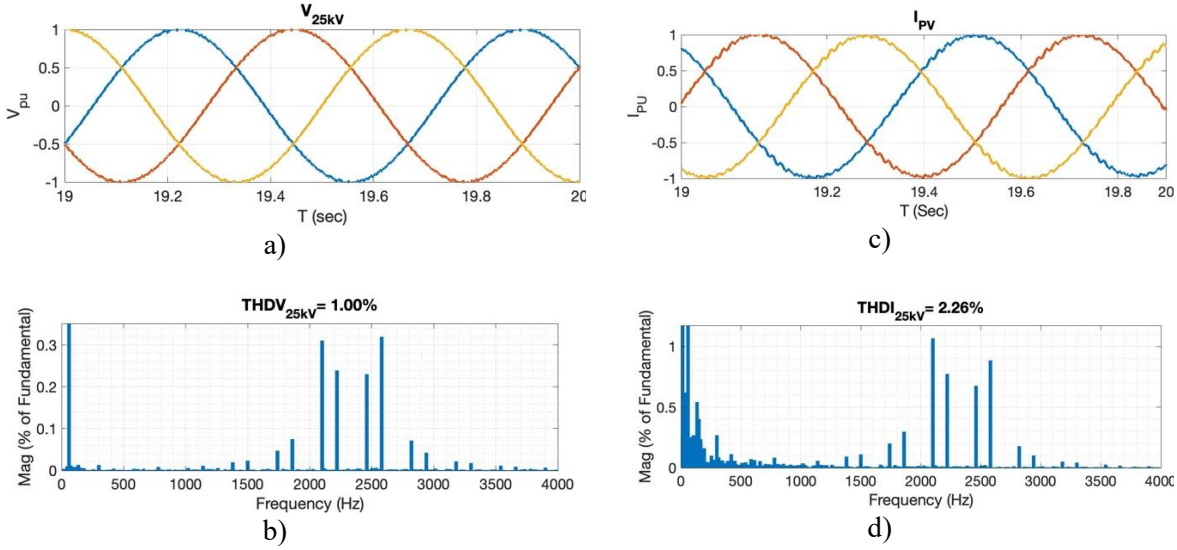

Figure 9: The (a) voltage waveforms, (b) voltage harmonic spectrums, (c) current waveforms and (d) current harmonic spectrums at the 25kV bus (PCC) for the system with the filter.

Table 8: The THDV (%), Vpu and THDI (%) values of the PV and 25 kV buses after filter installation.

THDV(%)	
25kV Bus	1.00 %
PV Bus	1.02 %
Vpu	
25kV Bus	1.02 p.u
PV Bus	1.03 p.u
THDI(%)	
25kV Bus	2.26 %
PV Bus	2.27 %

Table 8 presents the THDV (%), Vpu, and THDI (%) values of the PV and 25 kV buses after filter installation. In addition, Table 9 presents the individual THD performance of the source current and source voltage at the PV and 25 kV buses before compensation and after the application of the passive filter. Accordingly, after the connection of the LCL filter, the current and source voltage quality at the PV and 25 kV buses is improved compared to the previous case. Moreover, the THD values of voltage and current are reduced to below 1.02% and 2.26%, respectively, which are within the limits specified by IEEE 519.

Table 9: The Individual Total Harmonic Distortion values of voltage and current sources of PV and 25kV buses with and without filter application.

Harmonic Order	Current I_{25kV}		Voltage V_{25kV}		Current I_{PV}		Voltage V_{PV}	
	Without filter	***With Filter***	***Without filter***	***With Filter***	***Without filter***	***With Filter***	***Without filter***	***With Filter***
3rd	0.57%	0.207%	0.01%	0.006%	0.57%	0.2%	0.012%	0.11%
5th	1.73%	0.277%	0.07%	0.011%	1.73%	0.27%	0.072%	0.054%
7th	4.54%	0.077%	0.26%	0.004%	4.54%	0.077%	0.271%	0.017%
9th	0.15%	0.036	0.01%	0.002%	0.16%	0.036%	0.012%	0.014%
THD	10.65%	2.26	5.12%	1.00%	10.66%	2.27%	5.23%	1.02%

Lastly, at Table 10, cost and iteration values AOA algorithm to find optimal LCL filter parameters. For the LCL filter, cost values and iteration values are 0.1897 and 7 for the AOA algorithm, respectively. Also, to show the iterative process, Figure 10 is given below.

Table 10: For series LCL filter, the achieved cost and yield iteration numbers of the AOA algorithm.

	AOA
Cost	0.1897
Iter	7

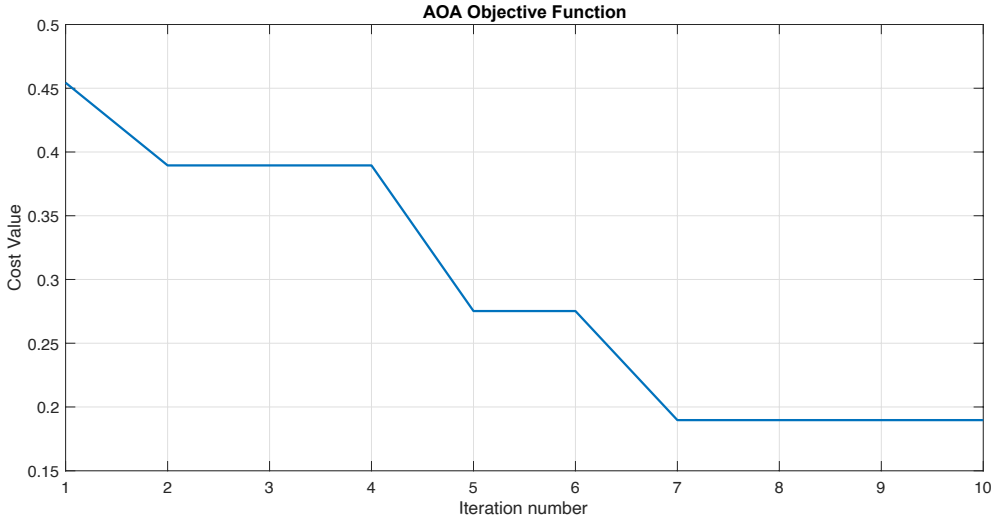

Figure 10: For series and shunt LCL filters, the objective function values obtained by AOA algorithm.

4.2. The analysis of FPV system with the optimal LCL filter under DD values

After the optimization process with AOA algorithm, the optimally designed LCL filter is connected to the FPV system. Also, to test the LCL filter, DD values for 30 days at same hour (10.00 AM) are used as input values (solar irradiance) of PV arrays. The daily representations of Vpu, THDV (%) and THDI (%) values are given in Figure 11.

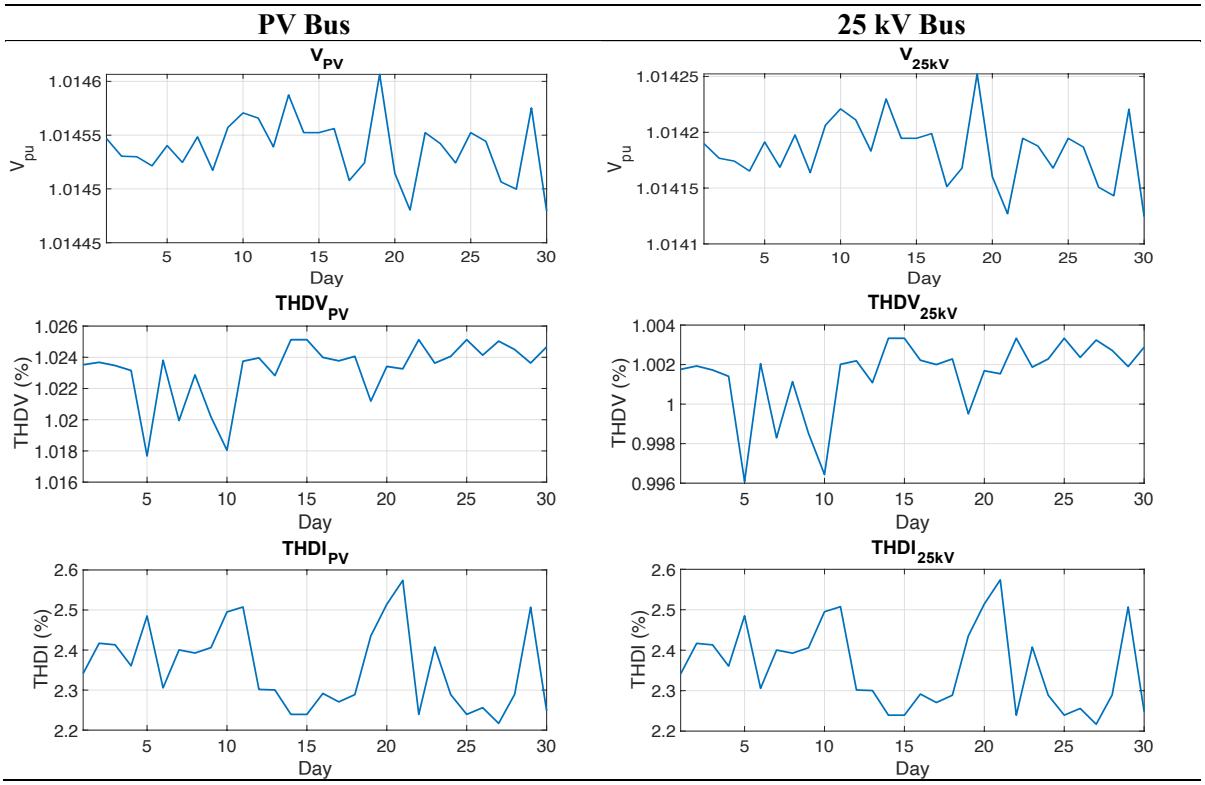

Figure 11: The comparative analysis of the Vpu, THDV, and THDI values for PV and 25 kV buses within the filtered FPV system will be conducted, with completion targeted within 30 days.

From Figure 9, for PV bus, THDV (%), THDI (%) and Vpu values change between 1.0177 %, 1.0251 %, 2.216 %, 2.57 % and 1.0145 p.u and 1.0146 p.u, respectively. Moreover, for 25kV bus, THDV (%), THDI (%) and Vpu values change between 0.996 %, 1.00 %, 2.216 %, 2.57 % and 1.0141 p.u and 1.0143 p.u, respectively. From these results, it can be concluded that, all parameters are kept between IEEE 519 standards. Also, it should be noted that, the optimally designed LCL filter from AM values successfully eliminates harmonic distortions in the system. Additionally, Vpu values are all close to the 1 p.u value for 30 days. Moreover, to demonstrate the boundaries of the system for DD values, Table 11 is given below.

Table 11: The min, mean and max values of THDV, THDI and Vpu indices for PV and 25 kV buses within 30 days.

			THDV	THDI	Vpu (p.u)
PV bus	Min	Value (%)	1.0177	2.2168	1.0145
		Day	5	27	30
		Solar Irradiation (W/m^2)	789	1023	1022
	Mean	Value (%)	1.0232	2.3557	1.0145
		-	-	-	-
		Solar Irradiation (W/m^2)	966.45	966.45	966.45
	Max	Value (%)	1.0251	2.5739	1.0146
		Day	14	21	19
		Solar Irradiation (W/m^2)	1029	926	889
25 kV (PCC) bus	Min	Value (%)	0.9961	2.2168	1.0141
		Day	5	27	30
		Solar Irradiation (W/m^2)	789	1023	1022
	Mean	Value (%)	1.00	2.3557	1.0142
		-	-	-	-
		Solar Irradiation (W/m^2)	966.45	966.45	966.45
	Max	Value (%)	1.00	2.5739	1.0143
		Day	14	21	19
		Solar Irradiation (W/m^2)	1029	926	889

As seen from Table 10, for PV bus, THDV (%) value is at its minimum with respect to the low solar irradiation (789 w/m^2) value at day 5. Also, the maximum value of THDV (%) is reached at day 14 with a high solar irradiation value (1029 W/m^2). Also, THDI (%) value is minimum with respect to the high solar irradiation (1023 W/m^2) value at day 27. Also, the maximum value of THDV (%) is reached on day 21 with a low solar irradiation value (1029 W/m^2). From the results, it can be said that high THDI values occur when PV inverters operate under light load conditions due to low solar insolation. Additionally, the Vpu value is minimal with respect to the high solar irradiation (1022 W/m^2) value at day 30. Also, the maximum value of Vpu is reached on day 19 with a low solar irradiation value (889 W/m^2). The related results are consistent because high solar irradiation means a high voltage value at the grid-side of the inverter.

Moreover, for the 966.45 W/m^2 solar irradiation value, the mean values (that means the AM value) of THDV (%), THDI (%) and Vpu, 1.02 %, 2.35 % and 1.014 p.u, respectively. These values are the improved versions of the unfiltered system (Table 5).

5. CONCLUSION

The study explores the implementation and optimization of a floating photovoltaic (FPV) system at Akköprü Dam, Muğla, Turkey, addressing a previously unexplored area in existing literature. By integrating a 2 MW FPV system with the local grid, the paper aims to leverage the benefits of FPV technology while addressing challenges related to harmonic distortions in voltage and current waveforms introduced by power electronics-based converters and inverters.

Key findings from the study include:

Motivation and Novelty:

- There is a growing interest in FPV systems in Turkey, but there is a lack of studies specifically addressing the application of FPV systems for Akköprü Dam.
- Previous research has examined various aspects of FPV systems in Turkey, such as analysis, capacity, shadow effects, and location proposals, but has not investigated the harmonic effects of FPV on the grid using daily data (DD). This study fills this gap by addressing harmonic analysis and optimal filter design using arithmetic mean (AM) data and performance analysis under DD.

Simulation and Design:

- The FPV system was simulated using AM values of DD obtained from the European Commission for Muğla, Turkey, ensuring the use of meteorological input data.
- An objective function (OF) was formulated, incorporating total harmonic distortion of the voltage waveform (THDV), the system's rms voltage levels, and harmonic distortion constraints, to guide the optimal design of series passive filters, specifically series LCL filters.
- The Antlion Optimization Algorithm (AOA), a recently proposed meta-heuristic optimization algorithm, was employed to determine the optimal parameters for the filter design problem.

Performance and Analysis:

- The FPV system, designed using real meteorological data from Akköprü Dam, Muğla, and simulated in Simulink, successfully demonstrated anticipated voltage and current waveforms.
- Optimal passive filter designs, particularly series LCL filters, were developed using the AOA algorithm to minimize THD and maintain power quality as per IEEE 519 standards.
- Comparative analysis between AM data and DD inputs revealed the robustness of the proposed filter designs in mitigating harmonic distortions and maintaining voltage levels within acceptable limits.

The analysis of the FPV system with the optimally designed LCL filter under daily data (DD) values over 30 days at Akköprü Dam demonstrates effective mitigation of harmonic distortions. The study used the Antlion Optimization Algorithm (AOA) to optimize the LCL filter, ensuring that total harmonic

distortion (THDV), current harmonic distortion (THDI), and per unit voltage (Vpu) values remained within IEEE 519 standards.

- For the PV bus, THDV ranged between 1.0177% and 1.0251%, THDI between 2.216% and 2.57%, and Vpu between 1.0145 and 1.0146 p.u.
- For the 25 kV bus, THDV ranged between 0.996% and 1.00%, THDI between 2.216% and 2.57%, and Vpu between 1.0141 and 1.0143 p.u.

These results confirm the LCL filter's effectiveness in maintaining power quality under varying solar irradiance conditions, demonstrating the system's robustness and stability. The study's findings indicate that high THDI occurs under low solar insolation, while high solar irradiation correlates with increased voltage values. The mean values for THDV, THDI, and Vpu with 966.45 W/m² solar irradiation were 1.02%, 2.35%, and 1.014 p.u., respectively, showcasing improvements over the unfiltered system. This comprehensive analysis validates the FPV system's performance and its potential for broader applications.

Also, this study is based on simulation results derived from a validated FPV–LCL filter model. Although the findings provide meaningful insights for reservoir-based FPV applications, experimental or hardware-in-the-loop validation was not included in the present work. Future research will focus on developing a small-scale prototype and performing real-time tests to further verify the proposed approach.

In conclusion, the paper outcomes indicate that the proposed FPV system, coupled with optimal filter designs, effectively mitigates harmonic distortions and enhances power quality. This provides a valuable contribution to the field of renewable energy systems. The successful implementation at Akköprü Dam sets a precedent for similar applications in Turkey and other regions, promoting sustainable energy solutions and environmental conservation.

Statement of Research and Publication Ethics

The study is complied with research and publication ethics.

Artificial Intelligence (AI) Contribution Statement

This manuscript was entirely written, edited, analyzed, and prepared without the assistance of any artificial intelligence (AI) tools. All content, including text, data analysis, and figures, was solely generated by the authors.

REFERENCES

[1] Y. A. Yusuf, “A comprehensive review of floating photovoltaic technology (FPVT) and its applications to improved efficiency,” J. Res. Technol. Eng., vol. 5, no. 3, pp. 71–77, 2024.

[2] R. C. González, “Energy production enhancement and evaporation reduction across 4,244 water bodies: performance evaluation of floating photovoltaic systems under diverse climates,” Renew. Energy, 2025.

[3] M. A. Manolache, “An evaluation of the efficiency of floating solar panels in Eastern Romania: assessing FPV potential in inland water bodies,” Ocean Eng., vol. 11, no. 1, art. 203, 2023.

[4] Department SD., Electricity Market Development Report 2017, Ankara, 2018.

[5] Republic of Türkiye Ministry of Energy and Natural Resources (MENR), “2023 Electricity Market and Installed Capacity Report,” Official Energy Statistics, Ankara, Türkiye, 2024.

[6] Yük Tevzi Dairesi Başkanlığı, Temmuz 2018 Kurulu Güç Raporu , Ankara, 2018.

[7] C. Yıldız, Offshore Solar Plants: A Design Study, (n.d.). https://doi.org/10.13140/RG.2.2.11727.36009.

[8] V. Vidović, G. Krajačić, N. Matak, G. Stunjek, M. Mimica, Review of the potentials for implementation of floating solar panels on lakes and water reservoirs, Renewable and Sustainable Energy Reviews 178 (2023). https://doi.org/10.1016/j.rser.2023.113237.

[9] A. Karadeniz, M.E. Balci, Comparative evaluation of common passive filter types regarding maximization of transformer’s loading capability under non-sinusoidal conditions, Electric Power Systems Research 158 (2018). https://doi.org/10.1016/j.epsr.2018.01.019.

[10] EU Science HUB, https://re.jrc.ec.europa.eu/pvg_tools/en/#TMY, (2024).

[11] C. Poongothai, K. Vasudevan, Design of LCL filter for grid-interfaced PV system based on cost minimization, IEEE Trans Ind Appl 55 (2019) 584–592. https://doi.org/10.1109/TIA.2018.2865723.

[12] S. Mirjalili, The ant lion optimizer, Advances in Engineering Software 83 (2015) 80–98. https://doi.org/10.1016/j.advengsoft.2015.01.010.

[13] M.K. Kaymak, A.D. Şahin, Problems encountered with floating photovoltaic systems under real conditions: A new FPV concept and novel solutions, Sustainable Energy Technologies and Assessments 47 (2021). https://doi.org/10.1016/j.seta.2021.101504.

[14] A.M. Ateş, Unlocking the floating photovoltaic potential of Türkiye's hydroelectric power plants, Renew Energy 199 (2022) 1495–1509. https://doi.org/10.1016/j.renene.2022.09.096.

[15] A.I. Manolache, G. Andrei, L. Rusu, An Evaluation of the Efficiency of the Floating Solar Panels in the Western Black Sea and the Razim-Sinoe Lagunar System, J Mar Sci Eng 11 (2023). https://doi.org/10.3390/jmse11010203.

[16] M.K. Kaymak, A.D. Şahin, The First Design and Application of Floating Photovoltaic (FPV) Energy Generation Systems in Turkey with Structural and Electrical Performance, International Journal of Precision Engineering and Manufacturing - Green Technology 9 (2022) 827–839. https://doi.org/10.1007/s40684-021-00369-w.

[17] A.M. ATEŞ, O.S. YILMAZ, F. GÜLGEN, Investigating the Effect of Shading on the Capacity Factor of Floating Photovoltaic Systems, Celal Bayar Üniversitesi Fen Bilimleri Dergisi 18 (2022) 309–319. https://doi.org/10.18466/cbayarfbe.1020070.

[18] E. Tercan, M.A. Dereli, B.O. Saracoglu, Location alternatives generation and elimination of floatovoltaics with virtual power plant designs, Renew Energy 193 (2022) 1150–1163. https://doi.org/10.1016/j.renene.2022.04.145.

[19] I. Gunes, R.S. Balog, Floating Solar Power Plant Applications in Turkey, in: 2024 IEEE Texas Power and Energy Conference, TPEC 2024, Institute of Electrical and Electronics Engineers Inc., 2024. https://doi.org/10.1109/TPEC60005.2024.10472178.

[20] E. Saad, S. Helmy, Y. Elkoteshy and U. AbouZayed, "Implementation of a Modified MPPT Strategy for Solar-PV Arrays Connected to Harmonic-Polluted Grids Under Partial Shading Conditions," 2021 International Telecommunications Conference (ITC-Egypt), Alexandria, Egypt, 2021, pp. 1-4, doi: 10.1109/ITC-Egypt52936.2021.9513923.

[21] Y. A. Yusuf, "A comprehensive review of floating photovoltaic technology (FPVT) and its applications to improved efficiency," J. Res. Technol. Eng., vol. 5, no. 3, pp. 71–77, 2024.

[22] R. C. González, "Energy production enhancement and evaporation reduction across 4,244 water bodies: performance evaluation of floating photovoltaic systems under diverse climates," Renew. Energy, 2025.

[23] J. Wu, X. Zhou, and M. Li, "Design and optimization of LCL filters for grid-connected converters in renewable energy systems: A global review," IEEE Access, vol. 11, pp. 128934–128952, 2023.

[24] Sharma and S. Bansal, "Global trends in floating photovoltaic installations and environmental performance," Solar Energy, vol. 256, pp. 145–159, 2023.

[25] M. Cengiz and T. Duman, "Design and analysis of L and LCL filters for grid-connected HNPC inverters used in renewable energy systems," Balkan Journal of Electrical and Computer Engineering, vol. 12, no. 1, pp. 53–61, 2024.

[26] N. Sarkarov and O. Karimzada, "LCL filter design and simulation for grid-connected PV systems" TechRxiv preprint, Feb. 2025.

[27] S. A. M. Sahana, A. M. K. Anusha, D. K. N. V. D. Kumar, U. M. Abhishek, and A. Joshi, "Simulation on optimisation of power quality using hybrid power system," International Research Journal of Engineering and Technology (IRJET), vol. 9, no. 7, pp. 1303–1308, Jul. 2022.

[28] EÜAŞ, Aegean Akköprü Dam Report 2023, Ankara, 2023. https://www.euas.gov.tr/santraller/akkopru-hes.

[29] EÜAŞ, https://www.euas.gov.tr/santraller/akkopru-hes, EUAŞ (2024).

[30] A. Karadeniz, M.E. Balci, S.H.E. Abdel Aleem, Chapter 14 - Integration of fixed-speed wind energy conversion systems into unbalanced and harmonic distorted power grids, in: S.H.E. Abdel Aleem, A.Y. Abdelaziz, A.F. Zobaa, R.B.T.-D.M.A. in M.P.S. Bansal (Eds.), Academic Press, 2020: pp. 365–388. https://doi.org/https://doi.org/10.1016/B978-0-12-816445-7.00014-1.

[31] IEEE standards, IEEE Standards 1547 Fuel Cells, Photovoltaics, Dispersed Generation, and Energy Storage, 2018.